Two-component scenario and related gaps in cuprates

N.Kristoffel*and P.Rubin
[1]Institute of Physics, University of Tartu, Riia 142, 51014 Tartu, Estonia

PACS. 74.72.-h High-T_c compounds – 74.20Mn Nonconventional mechanism
Cuprate interband model

Abstract. A simple model of cuprate superconductivity with an electron spectrum prepared by doping is developed. The pair-transfer interaction couples the itinerant band with two components ("hot" and "cold") of the defect subsystem. There are basic defect-itinerant gaps quenched by progressive doping. Band overlaps appear as novel sources for critical doping concentrations. Insulator to metal transitions in the normal state are expected here. Minimal quasiparticle excitation energies determine the pseudo- and superconducting gaps according to the doping-dependent disposition of bands. Two pseudogaps can be present at underdoping and two superconducting gaps can be manifested at overdoping. Various transformations and connections between the gaps agree qualitatively with versatile experimental findings. The superconducting density does not reflect the presence of "extrinsic" gaps because of the interband nature of the pairing. A Uemura type sublinear plot at underdoping with further recession is obtained. A mixed Fermi-liquid is restored near optimal doping where the chemical potential intersects all the band components. The metallization of the "cold" subsystem is essential for the rise of T_c on passing to optimal dopings.

*E-mail: kolja@fi.tartu.ee

1 Introduction

Extensive experimental data on superconductivity energetic characteristics have been collected for cuprates [1-14]. However, standardized measurements which cover self-consistently and smoothly the whole energy and doping scales are advisable. The presence of at least one superconducting gap and one or even of two pseudogaps [5-7], rises a question about the number of superconductivity order parameters. Indications of the appearance of two superconducting gaps can be found. The nature of the pseudogap which survives in the normal state has still remained debatable [15]. "Extrinsic" and "intrinsic" mechanisms have been proposed. In the latter case the pseudogap is caused by the fluctuating superconductivity order (preformed pairs) at $T > T_c$ and there is an immediate connection between the superconducting gap and the pseudogap. The extrinsic mechanism looks for the pseudogap source in the normal state electron spectrum. Bare gaps in it may be due by other type orderings (in lattice-phonon subsystem) or doping. At present such a type of explanation seems to be preferable [2].

A cuprate superconductor can be considered as a charge-transfer insulator perturbed by doping. In what follows the excitations in the charge channel will be considered. The excitations in the spin-subsystem build up an essential associated partner. Controversial statements on interrelations of cuprate gaps have been made. These concern transformations of superconducting gaps into pseudogaps on doping, the connection of superconducting and normal state gaps and the coexistence of various gaps in distinct doping regions. The authors believe that one way to reach a more physical insight into cuprate superconducting properties on the excitation-energy-doping phase diagram will be the elaboration of a simple (possibly partly postulative) model by using the general knowledge on these systems. The following comparison of the qualitative outcome with observations can then illuminate the background physics.

Cuprate superconductivity is widely discussed in the two-component scenario [16-18]. Its essence consists in the statement that a "defect-polaronic" subsystem bearing doped holes is functioning besides the itinerant valence band electrons. The framework of the two-component scenario leaves freedom for the precision of the nature of the electronic background and pairing channels. One can e.g. consider as basic ingredients a mainly oxygen band between the Cu-dominated Hubbard components and a distribution of states

created by doping [7,13,19-23] near the top of this band. Lattice effects enter this scenario through the inhomogeneous structure of CuO_2 planes in doped cuprates (stripes, tweed patterns, granularity) and the associated electronic phase separation [18,23-27].

Attempts to reflect the two-component scenario by a simple model have been started in [19,20,28-30]. The present contribution is a generalization, especially what concerns the superfluid density. Our model uses a nonrigid electronic playground of superconductivity prepared by doping. The "extrinsic" source of the pseudogaps lies in the bare normal state gaps between the defect and the itinerant states. These will be quenched with progressive doping. The mutual transformations between superconducting gaps and pseudogaps can be explained by the change of the nature of the minimal quasiparticle excitation energy on doping. The connection between pseudogaps and normal state gaps is due to the mixing of the normal state spectrum with the superconducting gaps in the quasiparticle energy expression. The fluctuation effects have not been taken into account in this model, cf. [15].

The electron spectrum considered in the two-component scenario is nonrigid. The appearance of a "defect" subsystem besides the itinerant one opens a novel channel for reaching high T_c-s by the interband pair transfer interaction [19, 20]. The corresponding two-band superconductivity mechanism [31, 32] has been known for a long time. A number of attempts [33] have been made to use it for cuprates in connection with the two-component scenario [19,20,26,28-30]. The interband pairing interaction operates in a considerable volume of the momentum space and works for pairing also as being repulsive. It also prevents the manifestation of normal state gaps in the superfluid density (order parameters) [19, 20].

2 The Model

A cuprate electron spectrum created and reorganized by doping is described as follows. The itinerant (valence) band (γ) states are lying between the energies $\xi = -D$ and $\xi(max) = 0$ and are normalized to $1 - c$. Here c is a measure of the doped hole concentration. It must be scaled for a given case, e.g. by joining characteristic concentrations on the phase diagram.

The defect subsystem is structurally anisotropic and this is manifested in different gap features over the momentum space [1-3,13,40]. The presence of

two pseudogaps [5-7] of different behaviour is impressive. The well-expressed large pseudogap is connected with the neighbourhood of the "hot" $(\pi, 0)$-type Brillouin zone points. The spectrum at $(\frac{\pi}{2}, \frac{\pi}{2})$-type "cold" points seems to be weakly gapped [40]. For these reasons the defect system will be characterized by two subbands for the "hot" (α) and "cold" (β) regions, cf [36]. These subbands occupy the energy intervals $d_1 - \alpha c$ and $d_2 - \beta c$, respectively, with the weight of states $c/2$. On underdoping these bands lie above the valence band. Note that the optical charge-transfer gap is reduced by doping [41]. A progressive doping brings first the β-band to overlap with the γ-band at $c_\beta = d_2\beta^{-1}$. A common overlapping distribution of all the bands starts at $c_\alpha = d_1\alpha^{-1}$. It is known that the infrared manifestation of the defect band is lost at larger dopings in favour of a Drude peak of (free) carriers [42].

The 2D (CuO_2 planes) densities of states of these bands read: $\rho_\gamma = (1-c)D^{-1}$; $\rho_\alpha = (2\alpha)^{-1}$; $\rho_\beta = (2\beta)^{-1}$ and $\beta < \alpha$ is supposed. There are three qualitatively different arrangements of the bands and the chemical potential (μ). At $c < c_\beta$ $\mu = d_2 - \beta c$ remains connected with the "cold" β-band. On underdoping the charge carriers are concentrated in this "cold" subsystem in accordance with [13]. For $c > c_\beta$, $\mu = (d_2 - \beta c)[1 + 2\beta(1-c)D^{-1}]^{-1}$ intersects both (β, γ)-bands. For the expressed dopings larger than c_0, determined by $d_1 - \alpha c_0 = \mu$, the role of the $(\pi, 0)$-type region increases essentially, cf. [43, 44]. Now the chemical potential $\mu = [\alpha d_2 + \beta d_1 - 2\alpha\beta c][\alpha + \beta + (1-c)2\alpha\beta D^{-1}]^{-1}$ intersects all the three overlapping bands.

The valence band is attributed to the hole-poor regions of the material. It remains the source of antiferromagnetic fluctuations whereas in the defect space distinct spin-structures can be built up (ferrons, polaron aggregates, etc.). Such type background has been used to describe the underdoped cuprate magnetic properties [37]. Presumably the defect part of the spectrum can be compared with the bosonic (bipolaronic) component of the theories including bozonization [37, 38].

3 Basic Expressions

The cuprate pairing mechanism will be described by the coupling of itinerant and defect subsystems through the pair transfer [33] interaction. Superconductivity is mutually induced in interacting components. The corresponding coupling constant W contains Coulombic and electron-phonon (repulsive)

contributions [33]. Pairs are formed from the particles of the same band.

The intraband contributions [33] are of less significance on the present level. The basic mean field Hamiltonian reads

$$H = \sum_{\sigma,\vec{k},s} \epsilon(\vec{k}) a^+_{\sigma\vec{k}s} a_{\sigma\vec{k}s} + \sum_{\vec{k}} \Delta_\gamma(\vec{k}) [a_{\gamma\vec{k}\uparrow} a_{\gamma-\vec{k}\downarrow} + a^+_{\gamma-\vec{k}\downarrow} a^+_{\gamma\vec{k}\uparrow}] - \sum_{\vec{k},\tau}{}^{\tau} \Delta_\tau(\vec{k}) [a_{\tau\vec{k}\uparrow} a_{\tau-\vec{k}\downarrow} + a^+_{\tau-\vec{k}\downarrow} a^+_{\tau\vec{k}\uparrow}] \; . \tag{1}$$

Here $\epsilon_\sigma = \xi_\sigma - \mu$, $\sigma = \alpha, \beta, \gamma$, $\tau = \alpha, \beta$ and $\sum^\tau$ means the integration with the densities of states $\rho_{\alpha,\beta}$ in the corresponding energy intervals. Usual designations are applicable for spins (s) and electron operators. The superconductivity order parameters are defined as

$$\begin{array}{rcl} \Delta_\gamma(\vec{q}) & = & 2 \sum_{\vec{k},\tau}^{\tau} W(\vec{q},\vec{k}) < a_{\tau\vec{k}\uparrow} a_{\tau-\vec{k}\downarrow} > \\ \Delta_\tau(\vec{q}) & = & 2 \sum_{\vec{k}} W(\vec{q},\vec{k}) < a_{\gamma-\vec{k}\downarrow} a_{\gamma\vec{k}\uparrow} > \; . \end{array} \tag{2}$$

The diagonalization of (1) yields the gap equation ($\Theta = k_B T$)

$$\begin{array}{rcl} \Delta_\gamma(\vec{q}) & = & \sum_{\vec{k},\tau}^{\tau} W(\vec{q},\vec{k}) \Delta_\tau(\vec{k}) E_\tau^{-1}(\vec{k}) th \frac{E_\tau(\vec{k})}{2\Theta} \\ \Delta_\tau(\vec{q}) & = & \sum_{\vec{k}} W(\vec{q},\vec{k}) \Delta_\gamma(\vec{k}) E_\gamma^{-1}(\vec{k}) th \frac{E_\gamma(\vec{k})}{2\Theta} \end{array} \tag{3}$$

with the usual form of the quasiparticle energies

$$E_\sigma(\vec{k}) = \sqrt{\epsilon_\sigma^2(\vec{k}) + \Delta_\sigma^2(\vec{k})} \; . \tag{4}$$

In what follows W will be taken as constant. Moreover $\Delta_\alpha = \Delta_\beta$ is set. At T_c, according to (3) the gaps Δ_σ tend simultaneously to zero. For $W > 0$ two s-type order parameters appear with the opposite signs [33]; expr. (1) uses positive Δ-s.

The number of paired carriers can be calculated as

$$n_s = \frac{1}{2} \left\{ \sum_{\vec{k}} \frac{\Delta_\gamma^2(\vec{k})}{E_\gamma^2(\vec{k})} th^2 \frac{E_\gamma(\vec{k})}{2\Theta} + \sum_{\vec{k}}{}^{\tau} \frac{\Delta_\tau^2(\vec{k})}{E_\tau^2(\vec{k})} th^2 \frac{E_\tau(\vec{k})}{2\Theta} \right\} \; . \tag{5}$$

Performing the integrations ($D, d > \Delta$) at zero temperature one finds for $c < c_\beta$

$$n_{s0} = \frac{1}{2} \left\{ \Delta_\alpha \rho_\beta \arctan \frac{\beta c}{\Delta_\alpha} + \Delta_\gamma \rho_\gamma \left[\frac{\pi}{2} - \arctan \frac{d_2 - \beta c}{\Delta_\gamma} \right] \right\} \; , \tag{6}$$

and for $c > c_\beta < c_0$

$$n_{s0} = \frac{1}{2}\left\{\Delta_\alpha\rho_\beta\left[\frac{\pi}{2} - \arctan\frac{d_2 - \beta c - \mu}{\Delta_\alpha}\right] + \Delta_\alpha\rho_\alpha\left[\frac{\pi}{2} - \arctan\frac{d_1 - \alpha c - \mu}{\Delta_\alpha}\right] + \right.$$

$$\left. + \Delta_\gamma\rho_\gamma\left[\frac{\pi}{2} - \arctan\frac{\mu}{\Delta_\gamma}\right]\right\} . \qquad (7)$$

It can be seen that the presence of the normal state gap $d_2 - \beta c$ does not prepare a fermionic gap in the superfluid density. At the critical concentration $c = c_\beta$ n_s remains continuous (the second term in (7) tends to zero).

4 The Gaps

Minimal quasiparticle energies reflect the presence of gaps in the excitation spectrum of the superconductor. This will be the case also for the pseudogaps, which appear naturally in the present model. The basic source lies here in the perturbative segregation of the fermionic subsystem by the presence and localization of the doped holes.

In the low underdoped region for $c < c_\beta$ one has

$$E_\alpha(min) = \Delta_l = \sqrt{(d_1 - \alpha c - \mu^2) + \Delta_\alpha^2}$$
$$E_\beta(min) = \Delta_\alpha \qquad (8)$$
$$E_\gamma(min) = \Delta_s = \sqrt{\mu^2 + \Delta_\gamma^2}\ . \qquad (9)$$

Further for $c > c_\beta$ and $c < c_0$ $E_\gamma(min)$ will be represented by Δ_γ as $\xi_\gamma = \mu$ can be satisfied. For $c > c_0$ also $E_\alpha(min)$ transforms to Δ_α.

In the normal state Δ_l and Δ_s survive and one interpretes these as pseudogaps. A pseudogap and the corresponding normal state gap are connected through the contribution of $\Delta_{\alpha,\gamma}$ into E_σ. At $T = T_c$, $\Delta_{\alpha,\gamma}$ vanish and the quasiparticle nature of the excitation is lost. Passing to the optimal doping the small pseudogap is smoothly transformed into the itinerant superconducting gap. The large pseudogap regime extends until $c \geq c_0$ is reached. The minimal excitation of the defect subsystem is further determined by the superconducting gap Δ_α. The connection and mutual transformation of

the pseudogap and the corresponding superconducting gap is based on the doping-variable structure of the spectrum which changes the nature of the minimal excitation energy of quasiparticles.

Concerning the manifestation of various gaps involved in the model, the valence band excitations belong to the "hot" spectrum. The "cold" spectrum is usually considered as nongapped [1-3,40]. If one accounts for the d-wave symmetry [40] by multiplying Δ_α with the corresponding symmetry function, the "cold" spectrum becomes empty. However, note that, depending on the doping level and temperature, the two-band model allowes pure d-, s- or mixed $d-s$ ordering symmetries [45]. Extreme dopings and low temperatures favour the s-wave nature. In spite of that the basic gap manifestations appear in the "hot" spectrum, the "cold" electrons act essentially in building up the superconductivity high T_c, supporting the interband pairing channel.

In summary the present model predicts the appearance of two pseudogaps on low dopings. Further the spectrum involves the large pseudogap and the itinerant superconducting gap. On overdoping the spectrum is expected to contain two superconducting gaps. Then the defect Δ_α will be manifested by an additional spectral weight inside of Δ_γ. In the case when the β-subsystem states overlap the itinerant band from the very beginning there will be only one (defect subsystem) pseudogap.

5 The Illustrations and Comparative Discussion

The theoretical cuprate phase diagram following from the present model is illustrated by Figures 1 and 2. The following plausible parameter set has been used: $D = 2$; $d_1 = 0.3$; $d_2 = 0.1$; $\alpha = 0.66$; $\beta = 0.33$ and $W = 0.28$ (eV). At this $T_c(max) = 125$ K is reached for $c = 0.57$ and $c_\alpha = 0.45$; $c_\beta = 0.38$; $c_0 = 0.57$. The scaling for a typical cuprate doping is made by $p = 0.28c$ according to the widely accepted value $p = 0.16$ corresponding to $T_c(max)$. The gaps in Fig.1 are given for $T = 0$ and the connections between them can be followed on the doping scale. There seems to be a general agreement with the findings for cuprates.

The expected common manifestation of two underdoped state pseudogaps has been established for the La- and Bi-cuprates [5-7]. Another class of com-

pounds with one charge channel pseudogap (bare nongapped β-subsystem) with the Δ_l-type behaviour is eventually possible. The smooth transformation of the small pseudogap into the larger superconducting gap (at p_β) has also been observed [5, 6, 13]. The large pseudogap extends to slight overdoping and then transforms into the defect system superconducting gap as has been found in Ref.[46]. Δ_l is attributed to the spectral hump-feature [9, 10]. On intermediate dopings Δ_l and the itinerant superconducting gap appear together. They cross close to the optimal doping. This corresponds to the observations [9]. Note that in a narrow doping region the larger superconducting gap exceeds the pseudogap Δ_l. The corresponding parameters of the itinerant and defect subsystem are not competing. Eventually, the hump is shifted to larger energies with reduced dopings as observed in [10] and it remains preserved for $T > T_c$ on the dopings where T_c is optimized [9].

Following the connection of the pseudogap with the "own" subsystem superconducting gap it can be seen that the manifestation of a superconducting gap on a given doping can be substituted by the appearance of the normal state gap (Fig.2) for $T > T_c$ in this region. It means that at low temperatures a pseudogap can remain not manifested on dopings where it will be found in the normal state (cf. [14]). In general the pseudogaps persist to $T = 0$. The rising temperature expands slightly the manifestation region of a pseudogap on the doping scale.

The manifestation of both superconducting gaps on overdoping is often debated. However the Fermi energy intersects the electron spectrum parts headed by different band components at different wave vectors and the larger Δ_γ can remain masked.

The temperature dependence of the pseudogaps remains at the present state of the model due by the contribution of the superconducting gaps. This leads to a slow diminishing with $T \to T_c$, whereas the superconducting gaps $\Delta_{\alpha,\gamma}$ reach zero at T_c in a "traditional" manner, cf. [47]. Figure 2 represents the behaviour of the superconducting density ($T = 0$) together with the normal state gaps and T_c. There are no signs of bare "extrinsic" fermionic gaps in a continuous curse of n_s and an argument [15] against the "extrinsic" source of the pseudogap fails. This is the result of the interband nature of the pairing. The normal- and pseudogaps and their large ratios to T_c rise dramatically with the diminishing of doping, whereby the superconducting gaps and density decrease.

In Fig.3 the calculated Uemura type [48] plot is shown. On underdoping

there is a sublinear segment connecting T_c and n_s with the further recession.

The dynamics of the band overlap in the present model introduces a novel source for special critical dopings. These correspond to the doping concentrations where the band components begin to overlap. The metallization of the cold defect-liquid is reached at c_β. On smaller dopings one supposes the formation of doped hole ferrons and a percolation type superconductivity [49]. The defect band acts as a bath of uncompensated spins. One can explain [37] the presence of a magnetic pseudogap [50, 51] in the spin excitation channel on such basis.

The hot defect subsystem metallizes at c_0 near the optimal doping. Here all the three bands of the model overlap and are intersected by the chemical potential. This means the built up of a common mixed Fermi liquid. The difference between the defect and the itinerant carriers is washed up. The large pseudogap gets lost when passing this border. Here one expects an insulator to metal transition in the normal phase. During the way to this concentration the Fermi surface becomes more and more electron like with peripheral hole pockets. Experiments on the normal phase [52] show that a quantum metal to insulator transition appears at a distinct c_k in the same region as c_0 lies. For smaller dopings the hot quasiparticles become insulating where the cold quasiparticles remain metallic. Various experimental findings add to the existence of a critical doping concentration in cuprates [21, 53, 54], where the properties of the electron liquid are essentially changed. Supposing that $c_k = c_0$, these findings become qualitatively explained. Such a c_k is of a basic importance in a quantum critical point scenario [53].

Some further essential properties of cuprates can be relatively simply explained by two-band models. The two observed electronic relaxation channels [46] and coherence lengths are a natural property of two-band superconductors [55].

The transition temperature and effective mass isotope effects can also be explained in two-band schemes [56, 57]. In general one observes a weak transition temperature effect for its optimal values and vice versa. This behaviour is caused by a contribution of a repulsive electron-phonon interaction in the whole pair-transfer scattering. This contribution of some percent in magnitude can cause the observed T_c-shifts. The pseudogap isotope effect [58] seems to be more complicated, being connected with the changes of both components in the quasiparticle energy.

The present simple model with plausability elements seems to be able to reproduce qualitatively the behaviour of energetic characteristics of cuprate superconductors. There remains a wide freedom to fill it in with better substantiated suppositions and quantitative aspects.

This work was supported by Estonian Science Foundation grant No 4961.

References

[1] T.Timusk, B.Statt, Rep. Progr. Phys. **62**, 61 (1999).

[2] T.Timusk, Solid State Commun. **127**, 337 (2003).

[3] A.Damascelli, Z.Hussain and Z.-X.Shen, Rev. Mod. Phys. **75**, 473 (2003).

[4] A.Mourashkine, Physica C **341**, 917 (2000).

[5] R.M.Dipasupil, J. Phys. Soc. Jpn. **71**, 1535 (2002).

[6] T.Sato, Physica C **341-348**, 815 (2000).

[7] A.Fujimori et al., Physica C **341-348**, 2067 (2000).

[8] A.T.Takahashi et al., J. Phys. Chem. Solids **62**, 41 (2001).

[9] V.M.Krasnov et al., Phys. Rev. Lett. **84**, 5860 (2000).

[10] N.Miyakawa et al., Phys. Rev. Lett. **83**, 1018 (1999).

[11] J.L.Tallon, J.W.Loram, Physica C **341-348**, 19 (2000).

[12] M.Moraghebi et al., Phys. Rev. B **63**, 214513 (2001).

[13] A.Ino et al., Phys. Rev. B **65**, 094504 (2002).

[14] Y.Ozyuzer et al., Europhys. Lett. **58**, 589 (2002).

[15] J.Stajic et al., Phys. Rev. B **68**, 024520 (2003).

[16] K.A.Müller, Physica C **341-348**, 11 (2000)

[17] D.Mihailovic, K.A.Müller, in: NATO ASI Materials Aspects of high-T_c Superconductivity, Kluwer, Dordrecht, 1997, p. 1-14.

[18] Stripes and Related Phenomena, Eds. A.Bianconi and N.Saini, Kluwer Acad. Publ., N-Y, 2000.

[19] N.Kristoffel and P.Rubin, Physica C **356**, 171 (2001).

[20] N.Kristoffel and P.Rubin, Eur. Phys. J. B **30**, 415 (2002).

[21] P.Schwaller et al., Eur. Phys. J. B **18**, 215 (2000).

[22] Y.Ando et al., Phys. Rev. Lett. **87**, 017001 (2001).

[23] C.C.Homes, Phys. Rev. B **67**, 184516 (2003).

[24] V.J.Emery and S.A.Kivelson, Physica C **219**, 597 (1993).

[25] J.Tranquada, J. Supercond. **9**, 397 (1997).

[26] A.Bianconi et al., Physica C **296**, 269 (1998).

[27] J.C.Phillips and J.Jung, Phil. Mag. B **81**, 745 (2001).

[28] N.Kristoffel and P.Rubin, Solid State Commun. **122**, 265 (2002).

[29] N.Kristoffel and P.Rubin, Int. J. Modern Phys. B **16**, 1739 (2002).

[30] N.Kristoffel and P.Rubin, Physica C **402**, 257 (2004).

[31] H.Suhl, B.T.Matthias and L.R.Walker, Phys. Rev. Lett. **3**, 552 (1959).

[32] V.A.Moskalenko, Fiz. Met. i Metalloved. **8**, 503 (1959).

[33] N.Kristoffel, P.Konsin and T.Örd, Rivista il Nuovo Cimento **17**, 1 (1994).

[34] L.P.Gorkov and A.V.Sokol, Pis'ma ZETF **46**, 333 (1987).

[35] A.Bussmann-Holder et al., J. Phys. Cond. Matter **13**, L169 (2001).

[36] A.Perali et al., Phys. Rev. B **62**, R9295 (2000).

[37] A.S.Alexandrov, P.P.Edwards, Physica C **331**, 97 (2000).

[38] R.Micknas, S.Robaszkiewicz and A.Bussmann-Holder, Physica C **387**, 58 (2003).

[39] N.Kristoffel, phys. stat. solidi b **210**, 195 (1998).

[40] C.C.Tsuei and J.Kirtley, Rev. Mod. Phys. **72**, 969 (2000).

[41] G.Zhao et al., Phys. Rev. B **63**, 132507 (2001).

[42] P.Calvani, phys. stat. solidi b **237**, 194 (2003).

[43] A.D.Gromko et al., Phys. Rev. B **68**, 174520 (2003).

[44] S.Sugai et al., Phys. Rev. B **68**, 184504 (2003).

[45] P.Konsin, N.Kristoffel and P.Rubin, phys. stat. solidi b **208**, 145 (1998).

[46] D.Mihailovic, Physica C **341-348**, 1731 (2000).

[47] P.Konsin, N.Kristoffel and P.Rubin, Solid state Commun. **97**, 567 (1996).

[48] Y.J.Uemura, in: Polarons and Bipolarons, Eds. E.K.H.Salje, A.S.Alexandrov and W.Y.Liang, Cambridge Univ., p. 453.

[49] V.Hizhnyakov, N.Kristoffel, E.Sigmund, Physica C **161**, 435 (1989).

[50] K.Kitazawa, Physica C **341-348**, 19 (2000).

[51] G.Deutcher, Nature **397**, 410 (1999).

[52] F.Venturini et al., Phys. Rev. Lett. **89**, 107003 (2002).

[53] D.Di Castro et al., Eur. Phys. J. B **18**, 617 (2000).

[54] W.Y.Liang, J. Phys. Cond. Matter **10**, 11365 (1998).

[55] T.Örd and N.Kristoffel, Physica C **331**, 13 (2000).

[56] P.Konsin, N.Kristoffel and T.Örd, Ann. d. Physik **2**, 279 (1993).

[57] T.Örd and N.Kristoffel, J. Low Temp. Phys. **117**, 253 (1999).

[58] D.T.R.Temprano et al., Phys. Rev. Lett. **84**, 1990 (2000).

Figure captions

Fig.1. Doping dependences of gaps: 1 – the large pseudogap Δ_l; 2 – the small pseudogap Δ_s; 3 – the itinerant system superconducting gap Δ_γ; 4 – the defect system superconducting gap Δ_α; 5 – T_c. $p = 0.28c$; $p_\alpha = 0.13$; $p_\beta = 0.085$; $p_0 = 0.16$; $p(T_{cm}) = 0.16$.

Fig.2. Doping dependences of the superconducting density (curve 1) and of the transition temperature (curve 2). Curves 3 and 4 represent the normal state gaps.Energetic characteristics are given in eV.

Fig.3. Transition temperature vs. the superconducting density (the Uemura plot).

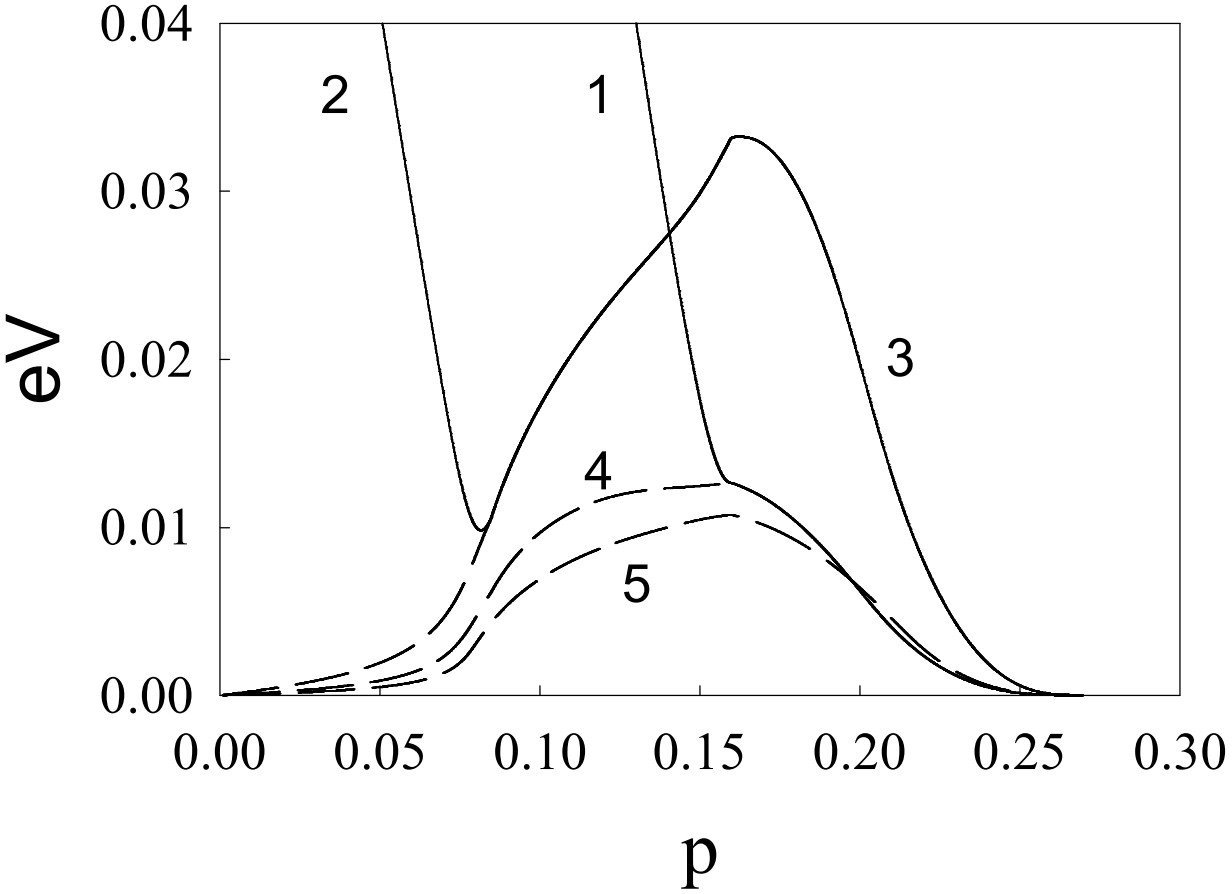
0.04
0.03
0.02
0.01
0.00
eV
0.00
0.05
0.10
0.15
0.20
0.25
0.30
p
1
2
3
4
5

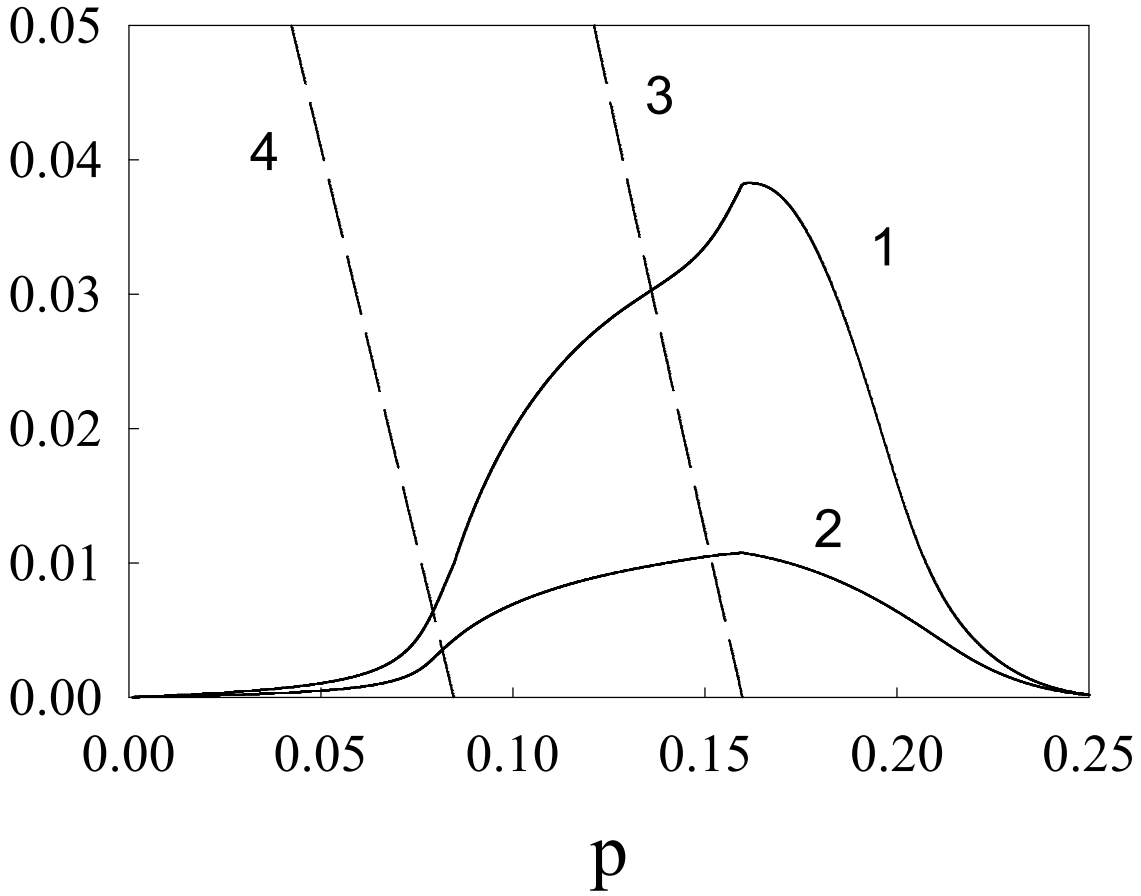
0.05
0.04
0.03
0.02
0.01
0.00
0.00
0.05
0.10
0.15
0.20
0.25
p
1
2
3
4

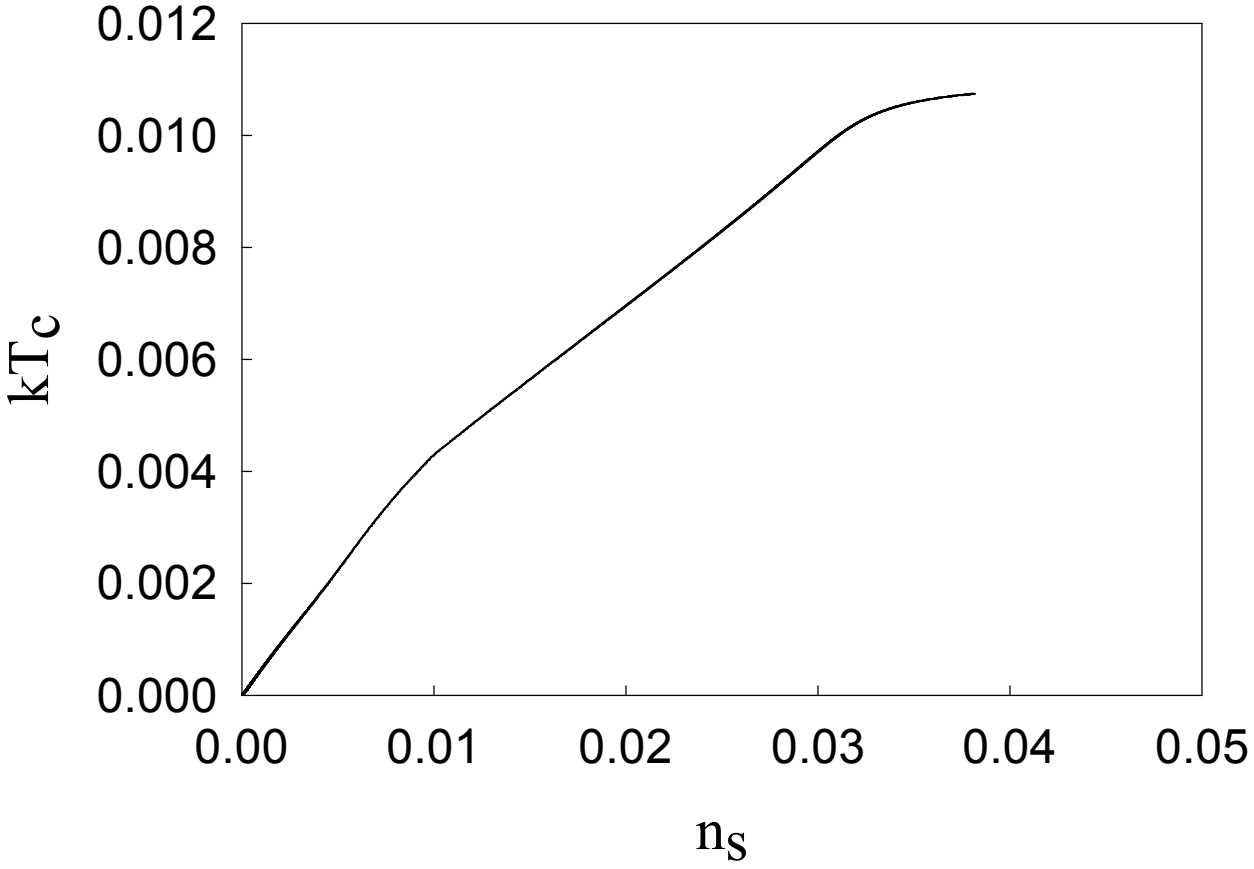
0.012
0.010
0.008
0.006
0.004
0.002
0.000
kTc
0.00
0.01
0.02
0.03
0.04
0.05
nS